Inorg. Chem. **1989**, *28*, 2181–2186

Contribution from the Department of Chemistry and Laboratory for Molecular
Structure and Bonding, Texas A&M University, College Station, Texas 77843

Reduction of $ReCl_5$ in the Presence of $PMePh_2$ To Give *mer*-$ReCl_3(PMePh_2)_3$, $ReCl(\eta^2-H_2)(PMePh_2)_4$, $ReH_3(PMePh_2)_4$, or $ReCl(CO)_3(PMePh_2)_2$, Depending on Conditions

F. Albert Cotton* and Rudy L. Luck

Received October 27, 1988

Reduction of $ReCl_5$ with excess magnesium in a THF/toluene (1:1) mixture in the presence of $PMePh_2$ leads to the formation of *mer*-$ReCl_3(PMePh_2)_3$ (**1**) in high yields. However, reduction with 4 equiv of Na affords $ReCl(\eta^2-H_2)(PMePh_2)_4$ (**2**), and when an excess of Na is employed, $ReH_3(PMePh_2)_4$ (**3**) is obtained. The complex $ReCl(CO)_3(PMePh_2)_2$ (**4**) is formed when solutions of **2** are placed under a CO atmosphere. The variable-temperature ^1H and ^{31}P NMR spectra of **2** and **3** are reported. The single-crystal X-ray structures of complexes **1** and **3** are reported. Crystal data: compound **1**, monoclinic, space group $P2_1/c$, $a = 11.429$ (3) Å, $b = 17.468$ (6) Å, $c = 23.189$ (6) Å, $\beta = 97.88$ (2)°, $V = 4585$ (7) Å^3, $Z = 4$, $R = 0.053$ ($R_w = 0.062$) for 365 parameters and 2424 unique data having $F_o > 3\sigma(F_o^2)$; compound **3**, triclinic, space group $P\bar{1}$, $a = 10.745$ (4) Å, $b = 22.136$ (4) Å, $c = 10.361$ (2) Å, $\alpha = 98.51$ (2)°, $\beta = 109.12$ (2)°, $\gamma = 98.38$ (2)°, $V = 2252$ (1) Å^3, $Z = 2$, $R = 0.054$ ($R_w = 0.093$) for 447 parameters and 7440 unique data having $F_o > 3\sigma(F_o^2)$. The geometry of **3** is that of a distorted pentagonal bipyramid with $PMePh_2$ ligands in the apical positions. The metal-bonded hydrogen atoms were located in the difference maps and refined to give an average Re–H distance of 1.76 [2] Å and a closest H–H distance of 1.96 (13) Å.

Introduction

There has been much interest in the chemistry of low-valent rhenium complexes containing tertiary phosphine ligands.[1] These complexes have been investigated in part because of their ability to bind dinitrogen[2] and, furthermore, because some have been shown to contain the molecular hydrogen ligand.[3] One of the most frequently employed preparative routes to synthesize rhenium hydride complexes entails the $LiAlH_4$ reduction of phosphine complexes of rhenium, e.g., $ReOCl_3(PPh_3)_2$.[4] More recently, sodium amalgam was utilized to reduce $ReCl_4(THF)_2$ in the presence of PMe_3 in THF under nitrogen to produce $ReCl(PMe_3)_5$ and $ReH(PMe_3)_5$.[5] In the case of PEt_2Ph, the dinitrogen complex $ReCl(N_2)(PEt_2Ph)_4$ is obtained.[5]

Here we describe how the products of the reduction of $ReCl_5$ in the presence of $PMePh_2$ under H_2 or Ar depend on the solvent used, the reducing agent employed (Mg vs Na/Hg), and the equivalents of reducing agent added. We find that *mer*-$ReCl_3(PMePh_2)_3$ (**1**) is obtained exclusively if Mg is used in a 1:1 THF/toluene solvent mixture. The molecular hydrogen complex $ReCl(\eta^2-H_2)(PMePh_2)_4$[3a] (**2**) is formed if exactly 4 equiv of Na/Hg is used in THF at 0 °C, and the trihydride $ReH_3(PMePh_2)_4$ (**3**) is obtained if an excess of Na and temperatures of ca. 50 °C are employed.

We also report the low-temperature ^1H and ^{31}P NMR spectra of complexes **2** and **3**, as well as the variable-temperature T_1 measurements on **3**. The X-ray single-crystal structures of **1** and **3** are also reported. Portions of this work were communicated earlier.[3a]

Experimental Section

General Data. All manipulations were carried out under either a dihydrogen or an argon atmosphere. Methanol was dried over magnesium methoxide, while other solvents were dried over sodium/potassium alloy and distilled under nitrogen before use. Tetrahydrofuran (THF) was further purified by distillation over $LiAlH_4$. $ReCl_5$ and $PMePh_2$ were used as purchased from Strem Chemical, Inc. The ^1H NMR spectra were recorded with Varian XL-200 and XL-400 spectrometers. ^{31}P NMR spectra, referenced externally to 85% H_3PO_4, were recorded at 81 MHz with a Varian XL-200 spectrometer. Electrochemical measurements were performed with a Bioanalytical Systems, Inc., Model BAS 100 electrochemical analyzer in conjunction with a Bausch and Lomb, Houston Instruments Model DMP 40 digital plotter. Experiments were carried out in a 0.2 M solution of tetra-*n*-butylammonium tetrafluoroborate in THF. A three-electrode cell configuration was used, with a glassy-carbon electrode (Model BAS MF 2012) and a platinum wire as working and auxiliary electrodes, respectively. A BAS MF 2020 Ag/AgCl cell was used as a reference electrode (against which ferrocene is oxidized at $E_{1/2} = +0.52$ V). All potentials were referenced to the Ag/AgCl electrode at 22 ± 2 °C. $E_{1/2}$ values were determined as $(E_{p,a} + E_{p,c})/2$. The microanalyses were done by Galbraith Laboratories, Inc., Knoxville, TN.

Preparation of $ReCl_3(PMePh_2)_3$ (1). $ReCl_5$ (0.3 g, 0.08 mmol) was added under Ar to a solution of $PMePh_2$ (0.7 mL, 3.5 mmol) dissolved in a mixture of 30 mL of THF and 30 mL of toluene. Iodine-activated magnesium (2.0 g) was then dumped into the reaction flask and the resulting mixture stirred at reflux temperature overnight. Unreacted magnesium was filtered off and the solvents removed under vacuo. The complex was extracted from the residue with benzene (30 mL) and the resulting solution filtered through Celite. The clear yellow-orange solution was concentrated to ca. 10 mL and MeOH (30 mL) added to effect the precipitation of yellow **1** (0.6 g, 84% yield). ^1H NMR (C_6D_6): δ 13.9 (d, 8 H, $J = 7$ Hz, *o*-Ph on $PMePh_2$ trans to $PMePh_2$ (abbreviated P-P)), 9.7 (d, 4 H, $J = 8$ Hz, *o*-Ph on $PMePh_2$ trans to Cl (abbreviated P-Cl)), 9.5 (t, 2 H, $J = 7.5$, *p*-Ph on P-Cl), 9.0 (t, 4 H, $J = 7.4$ Hz, *p*-Ph on P-P), 8.6 (t, 8 H, $J = 7.6$ Hz, *m*-Ph on P-P), 7.9 (t, 4 H, $J = 7.6$ Hz, *m*-Ph on P-Cl), –0.5 (s, 6 H, Me-P on P-P) –2.2 (s, 3 H, Me-P on P-Cl). ^{31}P NMR (THF): δ 38.6 (Br, P from P-Cl), –24 (Br, P from P-P). Anal. Calcd for $C_{39}H_{39}Cl_3Re$: C, 52.44; H, 4.40. Found: C, 52.62; H, 4.49.

Preparation of $ReCl(\eta^2-H_2)(PMePh_2)_4$ (2). $ReCl_5$ (1.0 g, 2.7 mmol) was added under H_2 to a solution of $PMePh_2$ (2.2 mL, 11.0 mmol) in THF (75 mL). A portion of Na amalgam (0.25 g of Na (11 mmol) in 3.5 mL of Hg) was then quickly poured into the reaction flask and the resulting solution stirred rapidly at 0 °C overnight. The yellow-brown solution was then filtered through Celite and concentrated to ca. 15 mL. The addition of 30 mL of methanol effected the precipitation of yellow **2** (1.6 g, 58% yield). The ^1H and $^{31}P\{^1H\}$ spectra of this complex were reported in ref 3a. Anal. Calcd for $C_{52}H_{54}ClP_4Re$: C, 60.96; H, 5.31. Found: C, 60.91; H, 5.45.

Preparation of $ReH_3(PMePh_2)_4$ (3). $ReCl_5$ (0.2 g, 0.6 mmol) was added under Ar to a solution of $PMePh_2$ (0.4 mL, 2.4 mmol) in THF (50 mL). Na amalgam (0.1 g of Na (4.3 mmol) in 10 g of Hg) was quickly poured into the flask and the mixture then placed under H_2. The mixture was stirred overnight at 50 °C, yielding a brownish solution. This solution was filtered through Celite and then concentrated under vacuum to ca. 5 mL. The addition of 20 mL of methanol effected the precipitation of the yellow product **3** (0.4 mg, 67% yield). ^1H NMR (CD_2Cl_2): δ 7.0–8.0 (m, 40 H, C_6H_5P), 1.2 (s, 12 H, CH_3P), –6.1 (q, 3 H, $J = 20$ Hz, *H*-Re); $^{31}P\{^1H\}$ NMR (CD_2Cl_2): δ –1.7 (s, 4 P, *P*-Re). ^{31}P NMR (CD_2Cl_2): δ –1.7 (q, 4 P, $J_{PH} = 19$ Hz, *P*-Re).

Preparation of $ReCl(CO)_3(PMePh_2)_2$ (4). A yellow-brown solution of complex **1** (0.125 g, 0.1 mmol) in benzene (10 mL) was placed under CO and stirred for 3 h at 50 °C. This resulted in a clear solution that was then concentrated to ca. 0.5 mL. The addition of 15 mL of methanol followed by rapid stirring and agitation resulted in the precipitation of

---

(1) Conner, K. A.; Walton, R. A. In *Comprehensive Coordination Chemistry*; Wilkinson, G., Gillard, R. D., McCleverty, J. A., Eds.; Pergamon: Oxford, U.K.; Vol. 4, pp 125–213.

(2) Chatt, J.; Dilworth, J. R.; Richards, R. L. *Chem. Rev.* **1978**, *78*, 589.

(3) (a) Luck, R. L.; Cotton, F. A. *J. Chem. Soc., Chem. Commun.* **1988**, 1277. (b) Luck, R. L.; Cotton, F. A. *Inorg. Chem.* **1989**, *28*, 6. (c) Costello, M. T.; Walton, R. A. *Inorg. Chem.* **1988**, *27*, 2563. (d) Crabtree, R. H.; Hamilton, D. G. *Adv. Organomet. Chem.* **1988**, *28*, 299.

(4) Chatt, J.; Coffey, R. S. *J. Chem. Soc. A* **1969**, 1963.

(5) Chiu, K. W.; Howard, C. G.; Rzepa, H. S.; Sheppard, R. N.; Wilkinson, G.; Galas, A. M. R.; Hursthouse, M. B. *Polyhedron* **1982**, *1*, 441.

0020-1669/89/1328-2181$01.50/0 © 1989 American Chemical Society

Table I. Crystallographic Data for $ReCl_3(PMePh_2)_3 \cdot C_6H_6 \cdot C_4H_8O$ (**1**) and $ReH_3(PMePh_2)_4$ (**3**)

formula	$C_{49}H_{53}Cl_3OP_3Re$	$C_{52}H_{55}P_4Re$
fw	1043.45	990.11
space group	$P2_1/c$	$P\bar{1}$
systematic absences	$0k0$, $k \neq 2n$; $h0l$, $l \neq 2n$	
a, Å	11.429 (3)	10.745 (4)
b, Å	17.468 (6)	22.136 (4)
c, Å	23.189 (6)	10.361 (2)
α, deg	90.0	98.51 (2)
β, deg	97.88 (2)	109.12 (2)
γ, deg	90.0	98.38 (2)
V, Å^3	4585 (7)	2252 (1)
Z	4	2
d_{calc}, g/cm^3	1.511	1.460
cryst size, mm	0.10 × 0.10 × 0.25	0.20 × 0.25 × 0.35
μ(Mo Kα), cm^{-1}	29.995	29.068
data collecn instrument	Nicolet P3/F equiv	Rigaku AFC5R
radiation (monochromated in incident beam)	Mo Kα (λ_a = 0.71073 Å)	
orientation rflns: no.; range (2θ), deg	25; 20–25	25; 43–48
temp, ±1 °C	19	19
scan method	ω	ω–2θ
data collecn range, 2θ, deg	$0 \leq 2\theta \leq 45$	$0 \leq 2\theta \leq 55$
no. of unique data, total with $F_o^2 > 3\sigma(F_o^2)$	3716, 2424	9815, 7440
no. of params refined	365	447
transmission factors, %: max, min	99.8, 94.0	100.0, 82.4
R^a	0.053	0.054
R_w	0.062^b	0.093^c
quality-of-fit indicator^d	1.06	1.74
largest shift/esd, final cycle	0.02	0.09
largest peak, e/Å^3	0.91	1.08

[a] $R = \sum||F_o| - |F_c||/\sum|F_o|$. [b] $R_w = [\sum w(|F_o| - |F_c|)^2/\sum w|F_o|^2]^{1/2}$; $w = 0.7145/\sigma^2[|F_o| + 0.001(F_o^2)]$. [c] $R_w = [\sum w(|F_o| - |F_c|)^2/\sum w|F_o|^2]^{1/2}$; $w = 2.7362/\sigma^2[|F_o| + 0.001(F_o^2)]$. [d] Quality of fit $= [\sum w(|F_o| - |F_c|)^2/(N_{observns} - N_{params})]^{1/2}$.

4 as a white powder (0.077 g, 90% yield). The IR, ^1H, and $^{31}P\{^1H\}$ spectra of this complex were reported in ref 3a. Anal. Calcd for $C_{29}H_{26}O_3ClP_2Re$: C, 49.33; H, 3.71. Found: C, 49.34; H, 4.08.

X-ray Crystallography. Suitable crystals of **1** and **3** were obtained by the slow diffusion of methanol into benzene solutions of **1** and **3**. All relevant crystallographic information is given in Table I. In both cases crystals were mounted on top of glass fibers with 5-min epoxy resin. Accurate unit cell parameters were obtained by means of a least-squares analysis of 25 reflections. Intensity data on each compound were then collected by utilizing the options specified in Table I and the general procedures for data collection as previously described.[6] All data sets were corrected for decay, Lorentz, and polarization effects. In addition, absorption corrections were also made by using an empirical method based on nine ψ scans (ψ = 0–360° every 10°) for χ values near 90°.[7] Nearly all of the non-hydrogen atoms were located from a three-dimensional Patterson function. Those remaining were found by alternating least-squares full-matrix cycles of refinement and difference Fourier maps for a cutoff ratio $F_o^2/\sigma(F_o^2)$ of 3. For this the Enraf-Nonius SDP software was employed. All of the non-hydrogen atoms were then refined anisotropically.

In the case of complex **1** two additional molecules were located in the difference maps: a THF molecule that originated from the preparation of **1** and a benzene molecule. Subsequent refinement on **1** was performed with the SHELX-76 package of programs. Hydrogen atoms were put in at calculated positions for the methyl groups and phenyl rings. The methyl groups were refined as rigid bodies, and the isotropic thermal parameters of the hydrogen atoms on the same carbon atom were constrained to the same value, which was refined. The phenyl groups were also refined as rigid bodies, and the thermal parameters on all of the hydrogen atoms attached to phenyl carbon atoms were constrained to the same value, which was refined. The atoms of the THF and benzene molecules were constrained to be a perfect pentagon and hexagon, respectively, and their respective isotropic thermal parameters constrained to the same values, which were refined. It was not possible to determine which one of the five atoms in the THF molecule was the oxygen atom, so only carbon atoms were used in this model.

Scheme I[a]

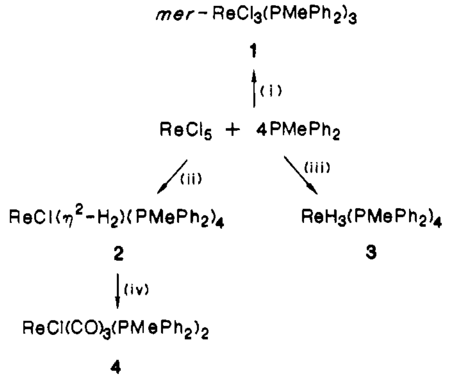

[a] Reaction conditions: (i) excess Mg, 50:50 THF/toluene solvent mixture, Ar, 100 °C; (ii) 4 equiv of Na/Hg, THF, Ar or H_2, 0 °C; (iii) excess Na/Hg, THF, Ar or H_2, 50 °C; (iv) benzene, CO, 50 °C.

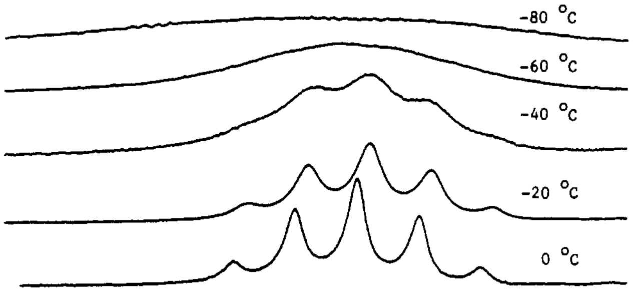

Figure 1. Variable-temperature ^1H NMR spectra of $ReCl(\eta^2\text{-}H_2)(PMePh_2)_4$ (**2**) in CD_2Cl_2 at 200 MHz.

The refinement method used on complex **3** was identical with that employed on **1**, except that the metal-bonded hydrogen atoms were refined freely. The final data are outlined in Table I. Tables listing the fractional atomic coordinates are available as supplementary material. Selected bond distances and angles are listed in Tables II and III, respectively.

Results and Discussion

Synthesis. Scheme I illustrates the reactions described in this paper. Complex **1** is formed in high yields in the Mg (excess) reduction of $ReCl_5$ in a 1:1 THF/toluene solvent mixture maintained at the reflux temperature in the presence of $PMePh_2$. If the reduction is carried out in pure THF, mixtures of complexes **1** and **2** are obtained.

To synthesize pure **2**, exactly 4 equiv of Na/Hg must be used as the reducing agent at 0 °C. This complex is of great interest, for it has been shown to contain a molecular hydrogen ligand.[3a] The reaction was done at low temperatures to favor the formation of **2** only and prevent the conversion of **2** into **3**. The trihydride complex **3** is obtained, in high yields, if excess Na/Hg is employed. Thus, the synthesis of the desired final product is determined by the nature of the solvent, the type and equivalents of reductant, and to some extent the temperature. As shown in Scheme I, complex **2** reacts under CO to form the complex *mer*-$ReCl(CO)_3(PMePh_2)_2$,[4] which has been characterized by IR, NMR, and analysis and by comparison to similar complexes.[8]

NMR Studies. The ^1H NMR spectra of complexes of the form $ReCl_3(PR_3)_3$ (PR_3 = PMe_2Ph, PEt_2Ph, P^nPr_2Ph, P^nBu_2Ph) have already been studied; these complexes were found to display sharp resonances, which was surprising because they are paramagnetic.[9]

---

(6) Bino, A.; Cotton, F. A.; Fanwick, P. E. *Inorg. Chem.* **1979**, *18*, 3558.

(7) North, A. C. T.; Phillip, D. C.; Matthews, F. S. *Acta Crystallogr., Sect. A: Cryst. Phys., Diffr., Theor. Gen. Crystallogr.* **1968**, *24A*, 351.

(8) (a) Bucknor, S.; Cotton, F. A.; Falvello, L. R.; Reid, A. H., Jr.; Schmulbach, C. D. *Inorg. Chem.* **1986**, *25*, 1021. (b) Hertzer, C. A.; Meyers, R. E.; Brant, P.; Walton, R. A. *Inorg. Chem.* **1978**, *17*, 2383.

(9) (a) Shaw, D.; Randall, E. W. *J. Chem. Soc. A* **1969**, 2867. (b) Chatt, J.; Leigh, G. J.; Mingos, D. M. P. *J. Chem. Soc.* **1969**, 1674. (c) Chatt, J.; Leigh, G. J.; Mingos, D. M. P.; Randall, E. W.; Shaw, D. *J. Chem. Soc., Chem. Commun.* **1968**, 419. (d) Gunz, H. P.; Leigh, G. J. *J. Chem. Soc. A* **1971**, 2229.

Table II. Selected Bond Distances and Angles for $ReCl_3(PMePh_2)_3$ (**1**)[a]

		Bond Distances (Å)			
Re–Cl(1)	2.349 (6)	Re–P(3)	2.470 (6)	P(2)–C(221)	1.85 (2)
Re–Cl(2)	2.446 (7)	P(1)–C(11)	1.83 (2)	P(2)–C(231)	1.82 (2)
Re–Cl(3)	2.344 (6)	P(1)–C(121)	1.82 (2)	P(3)–C(31)	1.81 (3)
Re–P(1)	2.448 (6)	P(1)–C(131)	1.85 (2)	P(3)–C(321)	1.77 (2)
Re–P(2)	2.474 (6)	P(2)–C(21)	1.81 (2)	P(3)–C(331)	1.84 (2)
		Bond Angles (deg)			
Cl(1)–Re–Cl(2)	93.9 (2)	Cl(3)–Re–P(3)	95.7 (2)	Re–P(2)–C(221)	121.8 (5)
Cl(1)–Re–Cl(3)	176.4 (2)	P(1)–Re–P(2)	98.1 (2)	Re–P(2)–C(231)	115.2 (6)
Cl(1)–Re–P(1)	94.0 (2)	P(1)–Re–P(3)	95.1 (2)	C(21)–P(2)–C(221)	97.0 (9)
Cl(1)–Re–P(2)	85.9 (2)	P(2)–Re–P(3)	165.8 (2)	C(21)–P(2)–C(231)	105.9 (9)
Cl(1)–Re–P(3)	87.8 (2)	Re–P(1)–C(11)	111.3 (8)	C(221)–P(2)–C(231)	103.6 (8)
Cl(2)–Re–Cl(3)	87.5 (2)	Re–P(1)–C(121)	121.5 (6)	Re–P(3)–C(31)	117.6 (9)
Cl(2)–Re–P(1)	172.1 (2)	Re–P(1)–C(131)	117.0 (6)	Re–P(3)–C(321)	116.5 (7)
Cl(2)–Re–P(2)	82.9 (2)	C(11)–P(1)–C(121)	103.2 (9)	Re–P(3)–C(331)	114.9 (6)
Cl(2)–Re–P(3)	84.9 (2)	C(11)–P(1)–C(131)	99 (1)	C(31)–P(3)–C(321)	105 (1)
Cl(3)–Re–P(1)	84.7 (2)	C(121)–P(1)–C(131)	101.8 (8)	C(31)–P(3)–C(331)	97 (1)
Cl(3)–Re–P(2)	90.9 (2)	Re–P(2)–C(21)	111.0 (8)	C(321)–P(3)–C(331)	103.0 (9)

[a] Numbers in parentheses are estimated standard deviations in the least significant digits.

Table III. Selected Bond Distances and Angles for $ReH_3(PMePh_2)_4$ (**3**)[a]

		Bond Distances (Å)			
Re–H(1)	1.81 (11)	P(1)–C(111)	1.838 (15)	P(3)–C(331)	1.85 (2)
Re–H(2)	1.72 (8)	P(1)–C(121)	1.873 (12)	P(3)–C(321)	1.806 (9)
Re–H(3)	1.75 (12)	P(1)–C(131)	1.850 (8)	P(3)–C(331)	1.846 (12)
Re–P(1)	2.354 (3)	P(2)–C(211)	1.803 (11)	P(4)–C(411)	1.818 (12)
Re–P(2)	2.361 (3)	P(2)–C(221)	1.856 (7)	P(4)–C(421)	1.839 (9)
Re–P(3)	2.376 (3)	P(2)–C(231)	1.871 (11)	P(4)–C(431)	1.846 (11)
Re–P(4)	2.388 (3)				
		Bond Angles (deg)			
H(1)–Re–H(2)	149 (5)	P(1)–Re–P(2)	160.1 (1)	C(211)–P(2)–C(221)	100.9 (5)
H(1)–Re–H(3)	140 (4)	P(1)–Re–P(3)	96.2 (1)	C(211)–P(2)–C(231)	100.5 (5)
H(1)–Re–P(1)	107 (4)	P(1)–Re–P(4)	94.1 (1)	C(221)–P(2)–C(231)	98.0 (4)
H(1)–Re–P(2)	93 (4)	P(2)–Re–P(3)	92.5 (1)	Re–P(3)–C(311)	115.6 (4)
H(1)–Re–P(3)	68 (3)	P(2)–Re–P(4)	92.0 (1)	Re–P(3)–C(321)	117.6 (3)
H(1)–Re–P(4)	68 (3)	P(3)–Re–P(4)	136.1 (1)	Re–P(3)–C(331)	119.7 (3)
H(2)–Re–H(3)	69 (4)	Re–P(1)–C(111)	121.5 (4)	C(311)–P(3)–C(321)	102.4 (6)
H(2)–Re–P(1)	81 (3)	Re–P(1)–C(121)	119.6 (3)	C(311)–P(3)–C(331)	100.7 (7)
H(2)–Re–P(2)	81 (3)	Re–P(1)–C(131)	115.0 (3)	C(321)–P(3)–C(331)	97.5 (5)
H(2)–Re–P(3)	142 (3)	C(111)–P(1)–C(121)	98.4 (7)	Re–P(4)–C(411)	115.7 (5)
H(2)–Re–P(4)	82 (3)	C(111)–P(1)–C(131)	100.9 (5)	Re–P(4)–C(421)	117.5 (3)
H(3)–Re–P(1)	86 (3)	C(121)–P(1)–C(131)	97.1 (4)	Re–P(4)–C(431)	118.5 (3)
H(3)–Re–P(2)	80 (4)	Re–P(2)–C(211)	121.7 (4)	C(411)–P(4)–C(421)	101.8 (6)
H(3)–Re–P(3)	73 (3)	Re–P(2)–C(221)	114.8 (2)	C(411)–P(4)–C(431)	101.6 (6)
H(3)–Re–P(4)	150 (3)	Re–P(2)–C(231)	117.1 (3)	C(421)–P(4)–C(431)	98.8 (5)

[a] Numbers in parentheses are estimated standard deviations in the least significant digits.

Table IV. T_1 Times for the Metal-Bonded Hydrogen Atoms in $ReH_3(PMePh_2)_4$ (**3**) at 400 MHz in CD_2Cl_2

temp, °C	T_1, ms[a]	temp, °C	T_1, ms[a]
22	280 (−6.1)	−49	142 (−6.2)
−9	208 (−6.1)	−69	192 (−6.2)
−29	191 (−6.1)	−89	247 (−5.9), 347 (−7.0)

[a] The chemical shift in ppm is given in parentheses after the T_1 values.

The ^1H NMR spectrum of **1** also contains sharp lines, and the peaks were tentatively assigned on the basis of their relative intensities and by comparison with literature assignments.[9c] It is interesting that we observed very broad resonances in the $^{31}P\{^1H\}$ NMR spectrum of **1**, in contrast to earlier observations, where no signals were obtained.[9a]

Some variable-temperature ^1H and $^{31}P\{^1H\}$ spectra of **2** are displayed in Figures 1 and 2, respectively. Previously, we showed how the low T_1 relaxation times (25 ms at −50 °C)[3a] for the metal-bonded hydrogen atoms at the different temperatures indicated that this was a molecular hydrogen (η^2-H_2) ligand.[10]

There are several more interesting points to be made about complex **2**. First, although the T_1 times for the metal-bonded hydrogen atoms fall into the range that would indicate an η^2-H_2 ligand (82 ms at 20 °C),[3a] the $^2J_{HP}$ coupling is very large (Figure 1, J = 19 Hz). Previously, such $^2J_{HP}$ couplings either were not observed or were shown through simulation to be very small (5.8 Hz).[3d,11] Second, the equilibrium between dihydride and η^2-H_2 forms that was clearly evident in the case of $W(CO)_3(P^iPr_3)_2H_2$[12] is not present in the case of **2**, as is evident in the ^1H NMR plots obtained from the T_1 studies. Furthermore, the η^2-H_2 ligand in **2** occupies a very "electron-rich" site, to judge from the ν_{NN} stretch (IR) of the dinitrogen analogue (ν_{NN} of $ReCl(N_2)(PMePh_2)_4$ 1925 cm^{-1}),[13] whereas ν_{NN} values for the previous dinitrogen analogues of η^2-H_2 complexes fall in the range 2060–2160 cm^{-1}.[14,15] Therefore, in **2**, the steric factors of the ancillary ligands play a very important role in stabilizing the H–H bond.[15] Finally, the low-temperature $^{31}P\{^1H\}$ NMR spectra display remarkable chemical couplings (Figure 2). At 78 °C the spectrum consists

---

[10] Hamilton, D. G.; Crabtree, R. H. *J. Am. Chem. Soc.* **1988**, *110*, 4126.

[11] Bautista, M.; Earl, K. A.; Morris, R. H.; Sella, A. *J. Am. Chem. Soc.* **1987**, *109*, 3780.

[12] Kubas, G. J.; Unkefer, C. J.; Swanson, B. I.; Fukashima, E. *J. Am. Chem. Soc.* **1986**, *108*, 7000.

[13] Chatt, J.; Dilworth, J. R.; Leigh, G. J. *J. Chem. Soc., Dalton Trans.* **1973**, 612.

[14] Morris, R. H.; Earl, K. A.; Luck, R. L.; Lazarowych, N. J.; Sella, A. *Inorg. Chem.* **1987**, *26*, 2674.

[15] Kubas, G. J. *Comments Inorg. Chem.* **1988**, *7*, 17.

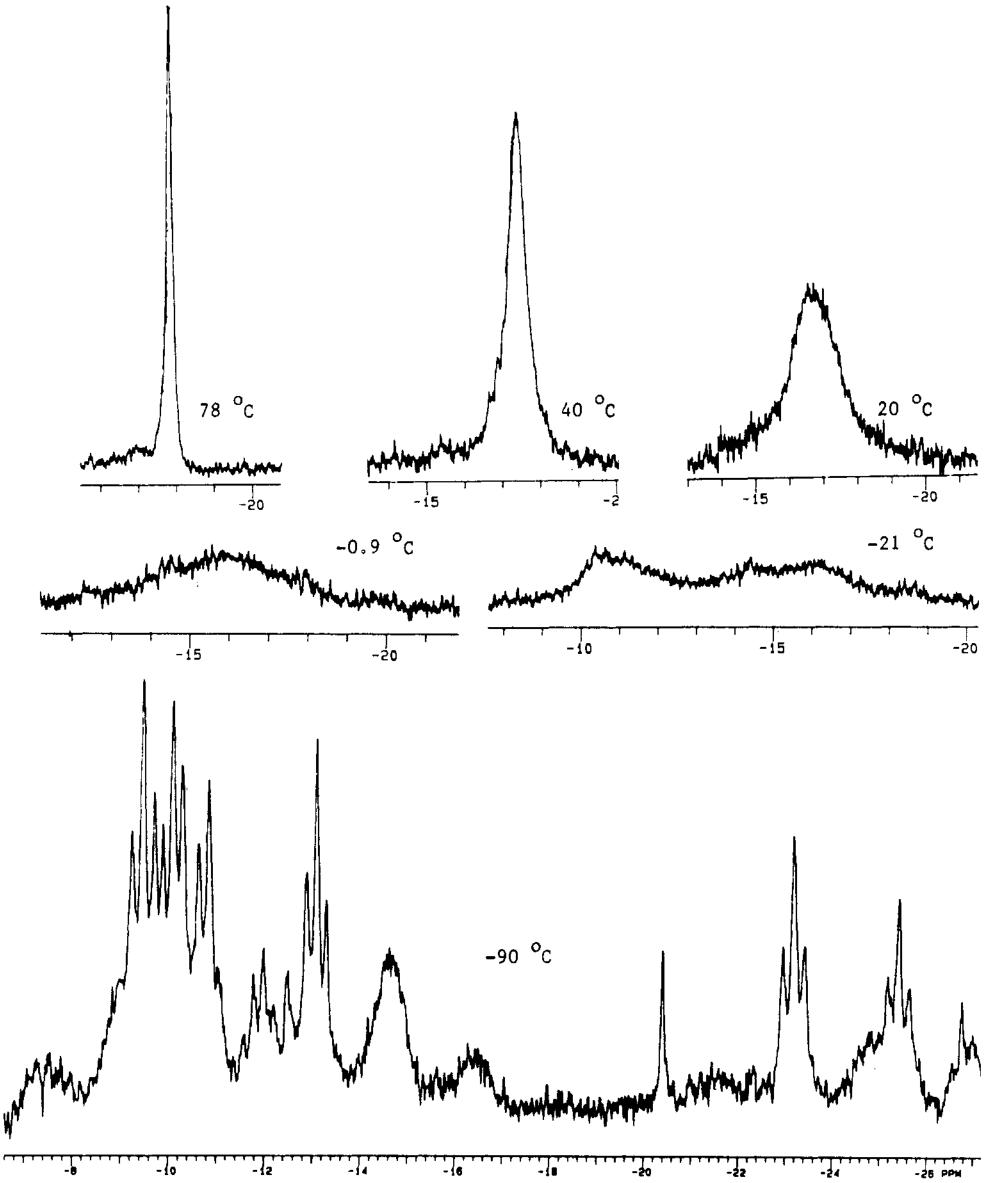

Figure 2. Variable-temperature $^{31}P\{^1H\}$ NMR spectra of $ReCl(\eta^2-H_2)(PMePh_2)_4$ (**2**) at 81 MHz. The solvent is CH_2Cl_2 when $T \leq 22$ °C and C_6H_6 when $T \geq 22$ °C.

of a sharp singlet, which is in keeping with four equivalent phosphorus atoms. However, a broad peak is obtained at room temperature, indicating some fluxional process is being frozen out, and at −21 °C at least two broad bumps are observed. At −91 °C various multiplets in the range of −27 to +7 ppm are observed. Only the multiplet at δ −17.9 is observed upon warming the solution to ca. 20 °C, indicating that this process is reversible. Furthermore, a coupled pattern is also observed at −91 °C in acetone for **2** in the presence of a large excess of $PMePh_2$. It is not clear exactly what process is responsible for this magnetic inequivalence of the phosphorus atoms. It is conceivable that either different rotamers of the phosphine ligands and/or different orientations of the η^2-H_2 ligand might be responsible.

Some variable-temperature ^1H NMR spectra for the hydride region only of complex **3** are displayed in Figure 3, and the T_1 times for these peaks are listed in Table IV. The spectrum at 22 °C consists as expected of a quintet (J = 20 Hz). This quintet becomes a very broad line at −70 °C, which is resolved into two bumps of 2:1 intensity of −80 °C. Finally at −105 °C the two bumps are further resolved into two overlapping triplets at ca. δ 5.86 and 5.90 (each with J = 22 Hz) and a triplet at δ 7.0 (J = 41 Hz). When the complex is warmed to ca. 20 °C, only the quintet at δ −6.1 is observed and, thus, this process is reversible. The X-ray single-crystal structure of **3**, discussed below, indicates that the geometry of **3** is that of a distorted pentagonal bipyramid. Thus, the two peaks in the hydride region can be assigned to the two different types of metal-bonded hydrogen atoms in the structure.

In a study on $ReH_3(dpae)_2$ (dpae = $Ph_2AsCH_2CH_2AsPh_2$) a similar ^1H NMR pattern in the hydride region was observed.[16] However, in this case the coupling was that of an A_2B pattern with J_{AB} = 9.5 Hz. This is much smaller than the two different coupling constants that we observed for **3**. In this case the observed pattern can best be described as due to each magnetically inequivalent hydrogen atom coupled to two equivalent phosphorus atoms with very small (not observed) couplings to the other two phosphorus atoms and also very small coupling to the other hydrogen atoms. Thus, in the case of **3** we have ^1H NMR evidence for two magnetically different phosphine ligands at low temperatures. This is also evident in the low-temperature $^{31}P\{^1H\}$ NMR spectra of **3**, where two bumps of roughly equal intensity are obtained at δ 5.8 and 4.0, at −90 °C.

Not shown in Figure 3 are the resonances due to the methyl groups on the $PMePh_2$ ligands, which change from a singlet (δ 1.2) at room temperature to two broad bumps (δ 0.2, 0.9) of equal intensity at −105 °C. This pattern is much simpler than the one obtained from the methyl groups in **2**, at ca. −90 °C, where several

---

(16) Ginsberg, A. P.; Tully, M. E. *J. Am. Chem. Soc.* **1973**, *95*, 4749.

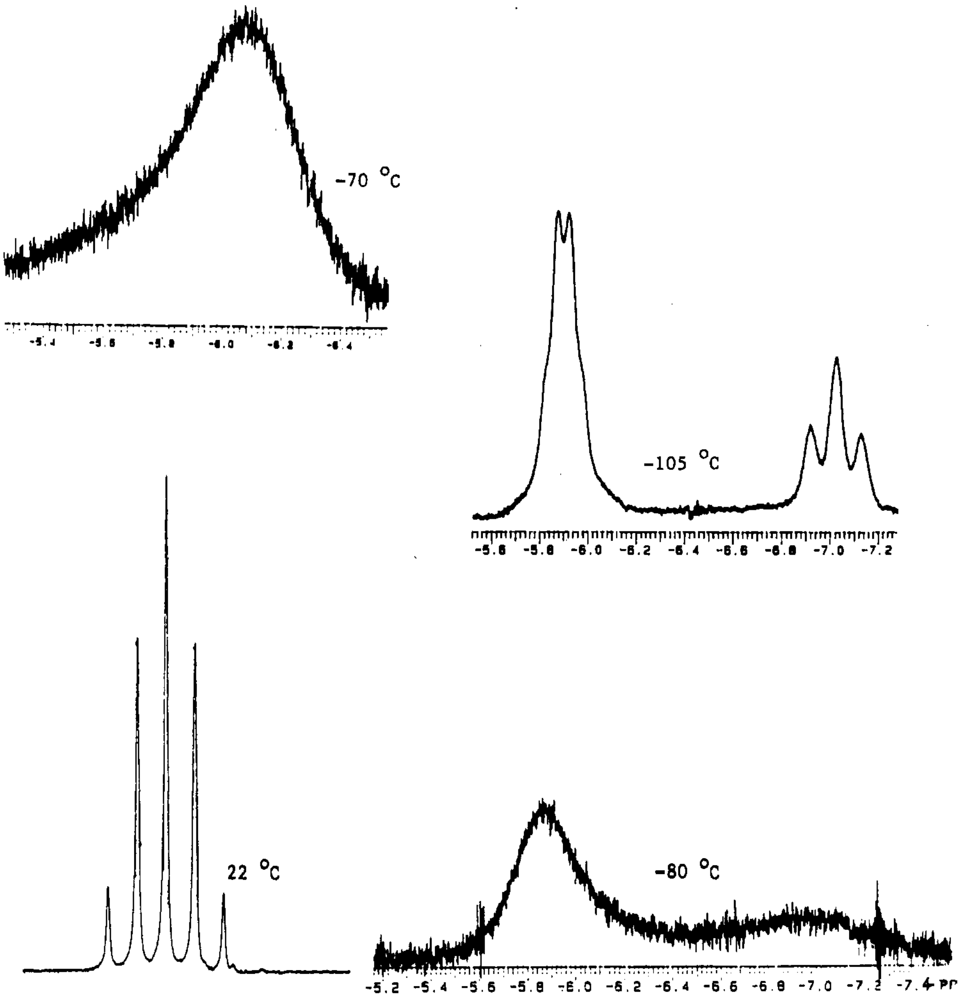

Figure 3. Variable-temperature ^1H NMR spectra of $ReH_3(PMePh_2)_4$ (**3**) in CD_2Cl_2 at 400 MHz. The quintet at 22 °C is at δ -6.06, with J = 20 Hz.

Table V. Electrochemical Data on Complexes 1–4

complex	$E_{1/2}(\text{ox})^a$
$ReCl_3(PMePh_2)_3$ (**1**)	0.9
$ReCl(\eta^2\text{-}H_2)(PMePh_2)_4$ (**2**)	-0.07
$ReH_3(PMePh_2)_4$ (**3**)	-0.17
$ReCl(CO)_3(PMePh_2)_2$ (**4**)	-0.17

[a] V vs Ag/Ag^+; 22 °C; solvent CH_2Cl_2; electrolyte $^nBu_4NBF_4$; scan rate 200 mV/s.

broad bumps not of equal intensity are observed in the range δ 0–2.

It is clear from these studies that in **3** we have a fluxional system which is resolved at -90 °C. The question that remains is whether or not this involves an equilibrium between a classical hydride and an η^2-H_2 ligand or three classical hydrides. The T_1 times listed in Table IV indicate a minimum value of 142 ms at 400 MHz and -49 °C, and this corresponds to a T_1(min) time of 71 ms at 200 MHz.[10,17] This is within the range reported for complexes possibly containing molecular hydrogen ligands (4–80 ms).[10] The T_1 times increase further as the temperature decreases, and then two different values are obtained for the unique hydride (347 ms) and the two geometrically equivalent ones (247 ms), in agreement with the previously described trends.[3b]

Electrochemical Data. Table V lists the oxidation potentials found for complexes **1**–**4**. As expected, complex **1** is the hardest to oxidize, consistent with this complex having the highest oxidation state. Complexes **2** and **3** are oxidized around -0.1 V vs Ag/AgCl, which is not surprising, but it is interesting that complex **4** would also be oxidized at a similar potential.

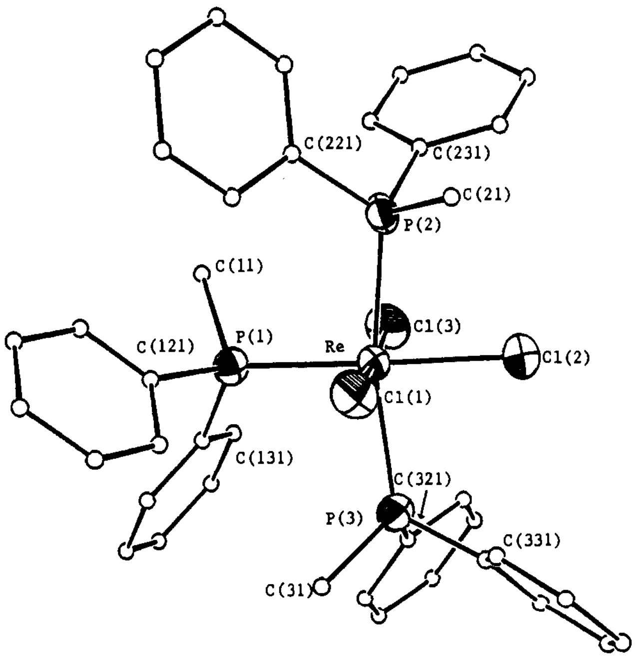

Figure 4. ORTEP drawing of **1**, with a partial listing of the atomic numbering scheme. the ellipsoids represent thermal displacements and are drawn at the 50% probability level. Carbon atoms are represented by spheres of arbitrary size.

Crystallographic Results. ORTEP drawings of complexes **1** and **3** are shown in Figures 4 and 5, respectively. Complex **1** exists

---

[17] Harris, R. K. In *Nuclear Magnetic Resonance Spectroscopy*; Pitman: London, 1983; pp 85–88.

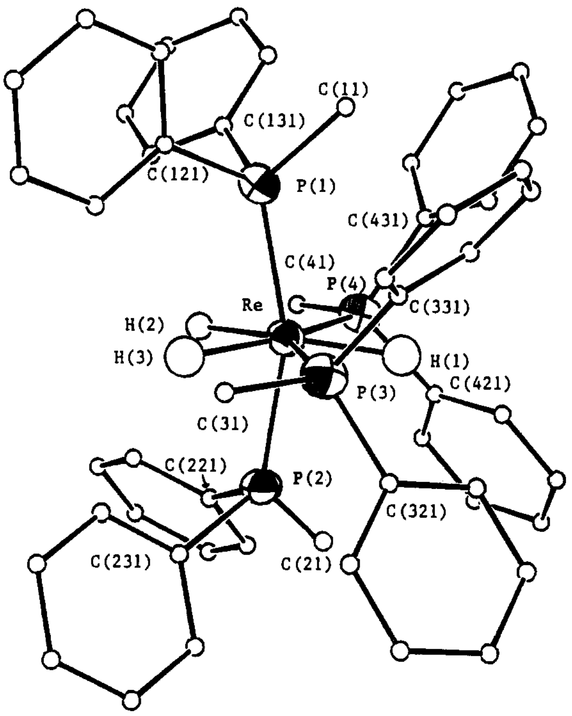

Figure 5. ORTEP drawing of **3**, with a partial listing of the atomic numbering scheme. Atoms H(1), H(2), and H(3) are represented by spheres based on their isotropic thermal parameters drawn at the 50% probability level. The remaining ellipsoids and spheres are as in Figure 4.

in the solid state in a meridional configuration. The same configuration was found in a crystallographic study[18] on the complex $ReCl_3(PMe_2Ph)_3$ (**5**), and this is also consistent with the solution studies discussed above. The average Re–Cl distances for Re–Cl(trans to Cl) (2.347 [3] Å)[19] and Re–Cl(trans to P) (2.446 (7) Å) are similar to those reported for **5** (2.353 (6) and 2.454 (6) Å, respectively). Furthermore, the average Re–P(trans to P) distances (2.472 [2] Å) are similar to those in **5** (2.458 (6) Å). However, there are significant differences between the Re–P(trans to Cl) distance in **1** (2.448 (6) Å) and that in **5** (2.401 (6) Å).

The geometry of complex **3**, as seen in Figure 5, is that of a distorted pentagonal bipyramid. The only other structure determinations on rhenium trihydrides have been on the complexes $ReH_3(dppe)_2$[20] (dppe = $Ph_2PCH_2CH_2PPh_2$) and $ReH_3(dppe)(PPh_3)_2$.[21] In these cases the metal-bonded hydrogen atoms were not located in the difference maps but it was pointed out that the overall geometry might be that of a pentagonal bipyramid. However, with **3** the metal-bonded hydrogen atoms were located in the difference maps and refined freely. The average Re–H distance of 1.76 [2] Å is about the same as those in $ReH_5(PMePh_2)_3$ (1.688 (5) Å)[22] and K_2ReH_9 (1.68 (1) Å)[23] which were determined by neutron diffraction. This is significant, because X-ray-determined metal–hydride distances should be shorter than those obtained by neutron diffraction. Furthermore, the H(2)–H(3) distance of 1.96 (13) Å is much longer than would be expected if this complex were to be classified as containing a molecular hydrogen ligand (where $d(\text{H–H}) < 1.2$ Å).[24] Of course, one possibility that cannot be ruled out is that the structure was done on an isomer that contained only classical hydride ligands. However, if one assumes that this is an adequate structural representation of **3**, then there must be some other explanation for the short T_1 values obtained. In addition to the dipole–dipole mechanism there are other relaxation processes that might be responsible for the short T_1 times measured,[25] but they have not previously been invoked in such compounds.

The interesting angles in complex **3** are those of P(3)–Re–P(4) (136.08°) and P(1)–Re–P(2) (160.05°), where P(1) and P(2) are bent toward the smaller H(2) and H(3) ligands and away from the two bulky equatorial phosphine groups. The Re–P average distance of 2.370 [8] Å is similar to those reported for $ReH_3(dppe)_2$[20] (2.34 Å) and $ReH_3(dppe)(PPh_3)_2$[21] (2.36–2.39 Å).

Conclusions. The direct reduction of $ReCl_5$ in the presence of phosphines is a good synthetic route to low-valent rhenium complexes. The products obtained depend on the choice of reducing agent and reaction conditions. The H(2)–H(3) distance of 1.96 (13) Å determined in a structural analysis of $ReH_3(PMePh_2)_4$ (**3**), if it is accurate, provides further evidence that the upper limit of the range (currently 4–80 ms at 200 MHz)[10] used in the NMR T_1 method to ascertain whether a molecule contains a nonclassical dihydrogen ligand is too high. We suggest, in the case of polyhydride complexes, that such conclusions be drawn only if supported by solid-state structural characterizations, of which the neutron structure would be the most definitive.

Acknowledgment. We thank the National Science Foundation for financial support.

Supplementary Material Available: ORTEP drawings with full atomic numbering schemes, stereoviews of unit cell packings, and tables listing all fractional atomic coordinates, positional parameters for hydrogen atoms, bond distances and angles, and anisotropic displacement parameters for complexes **1** and **3** (36 pages); listings of observed and calculated structure factors for **1** and **3** (58 pages). Ordering information is given on any current masthead page.

---

(18) Aslanov, L.; Mason, R.; Wheeler, A. G.; Whimp, P. O. *J. Chem. Soc. D* **1970**, 30.

(19) Brackets signify the variance, viz. $[(\sum \Delta_i^2)/n(n-1)]^{1/2}$.

(20) Albano, V. G.; Bellon, P. L. *J. Organomet. Chem.* **1972**, *37*, 151.

(21) *Chem. Abstr.* **1968**, *69*, 39504s.

(22) Emge, T. J.; Koetzle, T. F.; Bruno, J. W.; Caulton, K. G. *Inorg. Chem.* **1984**, *23*, 4012.

(23) Abrahams, S. C.; Ginsberg, A. P.; Knox, K. *Inorg. Chem.* **1964**, *3*, 558.

(24) Hampton, C.; Cullen, W. R.; James, B. R.; Charland, J.-P. *J. Am. Chem. Soc.* **1988**, *110*, 6918.

(25) Ellis, P. D. Private Communication.